

4-25-2006

Highly coercive rapidly solidified Sm–Co alloys

Shampa Aich

University of Nebraska - Lincoln, saich2@unl.edu

V.K. Ravindran

University of Nebraska - Lincoln

Jeffrey E. Shield

Iowa State University, jshield@unl.edu

Follow this and additional works at: <http://digitalcommons.unl.edu/cmrafacpub>



Part of the [Nanoscience and Nanotechnology Commons](#)

Aich, Shampa; Ravindran, V.K.; and Shield, Jeffrey E., "Highly coercive rapidly solidified Sm–Co alloys" (2006). *Faculty Publications from Nebraska Center for Materials and Nanoscience*. Paper 7.

<http://digitalcommons.unl.edu/cmrafacpub/7>

This Article is brought to you for free and open access by the Materials and Nanoscience, Nebraska Center for (NCMN, formerly CMRA) at DigitalCommons@University of Nebraska - Lincoln. It has been accepted for inclusion in Faculty Publications from Nebraska Center for Materials and Nanoscience by an authorized administrator of DigitalCommons@University of Nebraska - Lincoln.

Highly coercive rapidly solidified Sm–Co alloys

S. Aich,^{a)} V. K. Ravindran, and J. E. Shield

Department of Mechanical Engineering and Center for Materials Research and Analysis, N104, WSEC, University of Nebraska, Lincoln, Nebraska 68588

(Presented on 31 October 2005; published online 25 April 2006)

Highly coercive (H_c up to 37 kOe at 300 K), high remanent permanent magnets have been achieved by rapid solidification of binary Sm–Co alloys and Sm–Co alloys modified with Nb and C. Rapidly solidified SmCo_x alloys with x ranging from 5 to 11.5 formed predominantly a solid solution TbCu_7 -type SmCo_7 phase, although hcp Co was observed for $x > 7.3$. A coercivity value of 10 kOe was observed for $x < 6.1$, even though the microstructural scale was on the order of $1 \mu\text{m}$. The coercivity decreased significantly with the presence of the hcp Co phase, which formed initially as $\sim 80 \text{ nm}$ grains and, at higher x , as primary dendrites. Additions of 3 at. % Nb or 3 and 5 at. % C profoundly affected the coercivity values. Transmission electron microscopy (TEM) investigations revealed the origin of the improved coercivity. The addition of Nb resulted in a significant reduction in microstructural scale. The SmCo_7 grain size decreased systematically with Nb content, reaching 150–200 nm at 3 at. % Nb. The addition of C also significantly enhanced the coercivity, which systematically increased with C content and reached 37 kOe at 5 at. % C. The effect of C, however, resulted in morphological changes as TEM revealed the formation of an intergranular phase that effectively isolated the hard magnetic SmCo_7 grains from one another, reducing magnetic interactions. Excellent isotropic energy products of 6–8 MGOe were also achieved. © 2006 American Institute of Physics. [DOI: 10.1063/1.2173238]

INTRODUCTION

There is a great deal of interest in developing coercivity in Sm–Co-based permanent magnets through simpler processing. For example, rapid solidification effectively forms the TbCu_7 -type metastable structure from which precipitation-hardened magnets derive their microstructures upon appropriate heat treatment.^{1–4} Efforts to produce improved magnetic properties in as-solidified Sm–Co alloys would eliminate the need for additional processing. Very high coercivity ($\sim 40 \text{ kOe}$) was observed in melt-spun Sm–Co.^{5,6} These alloys, however, relied on significant amounts of alloying additions to produce the proper solidification behavior necessary to obtain the high coercivity. Efforts to produce high coercivities without alloying additions have produced only modest results.⁷ Here, we have investigated the role of Sm/Co ratio on the magnetic properties and also reported significant improvements in coercivity with only minor alloying additions.

EXPERIMENTAL PROCEDURES

Three series of alloys have been examined in this study. The first series were simple binary Sm–Co alloys with varying Sm/Co ratios; these had a nominal composition of SmCo_x with x ranging from 5 to 11.5. The other series examined a fixed Sm/Co ratio with Nb or C additions, with nominal compositions of $(\text{SmCo}_{7.3})_{100-y}T_y$, where $T = \text{Nb}$ or C and $y = 3$ and 5 . The alloys were made from high purity ($>99.95\%$) elemental constituents by arc melting in a high purity argon atmosphere. Before arc melting, 5% extra Sm

was added to the sample to compensate for loss due to Sm vaporization during melting. The ingot was then rapidly solidified by melt spinning in high purity argon at a chamber pressure of 1 atm and a tangential wheel velocity of 40 m/s.

The magnetic measurements were made by superconducting quantum interference device (SQUID) magnetometry at 300 K utilizing a Quantum Design MPMS with a maximum field of 7 T. Magnetic measurements were made on several ribbon pieces mounted so that the magnetic field was applied in the plane of the ribbon. Transmission electron microscopy was accomplished with a JEOL2010 operating at 200 kV. Electron transparency was achieved by mounting the melt-spun ribbon on a slightly polished Cu oval and by ion milling to perforation using a Gatan Duomill or precision ion polishing system (PIPS) at 4.5 kV. Structural characterization by x-ray diffraction was also conducted using a Philips diffractometer and $\text{Cu } K\alpha$ radiation.

RESULTS AND DISCUSSIONS

X-ray diffraction and microscopic observation revealed that rapid solidification of the binary SmCo_x alloys with x

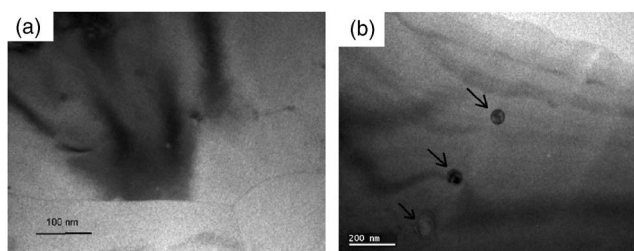


FIG. 1. Transmission electron micrographs revealing the microstructure of the SmCo_x alloy melt spun at 40 m/s (a) for $x = 6.1$, showing only large 1:7 grains, and (b) for $x = 7.3$, showing large 1:7 grains and scattered Co precipitates.

^{a)}Author to whom correspondence should be addressed; electronic mail: saich2@unlserve.unl.edu

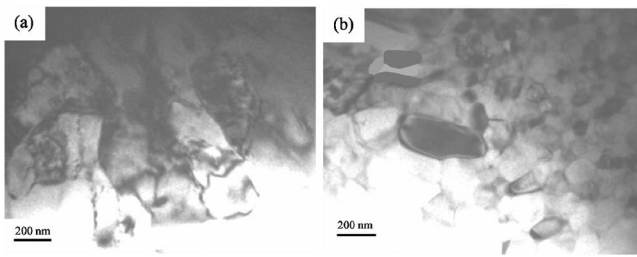


FIG. 2. Transmission electron micrographs revealing the microstructure of (a) the $(\text{Sm}_{0.12}\text{Co}_{0.88})_{97}\text{Nb}_3$ alloy melt spun at 40 m/s, showing equiaxed smaller 1:7 grains, and (b) the $(\text{Sm}_{0.12}\text{Co}_{0.88})_{97}\text{C}_3$ alloy melt spun at 40 m/s, showing a mixture of equiaxed grains having a wide range of size distribution.

ranging from 5 to 11.5 resulted in the formation of only the SmCo_7 phase with the TbCu_7 -type structure for $x < 7.3$, and for $x \geq 7.3$ a two-phase mixture of the SmCo_7 phase and Co was observed. The rapid solidification effectively suppressed the formation of the equilibrium $\text{Sm}_2\text{Co}_{17}$ phase with the $\text{Th}_2\text{Zn}_{17}$ -type structure. However, the rapid solidification resulted in only modest refinement of the microstructural scale. Figure 1 shows the transmission electron micrographs of the SmCo_x with $x=7.3$ and 6.1. The grain size of the SmCo_7 phase was observed to be on the order of $1 \mu\text{m}$ for all SmCo_x alloys with $x < 11.5$, which is rather coarse considering the processing route. The other binary alloys formed a variety of microstructures.⁸ Also notable in the Fig. 1(b) is the presence of a second phase, which electron diffraction revealed to be fcc Co.

Alloying to form $(\text{SmCo}_{7.3})_{97}\text{T}_3$ with $T=\text{C}$ and Nb eliminated the fcc Co formation, as neither x-ray diffraction nor microscopic examination revealed any fcc Co. However, both alloying additions resulted in a refinement in the grain size (Fig. 2). Both Nb and C additions of 3 at. % reduced the grain size to 150–200 nm. However, the C addition resulted in the formation of a second phase along the grain boundaries. No similar second phase was observed for the alloy with the Nb addition. An alloy with a higher level of C addition (5 at. %) was examined as well. The higher concentration had a dramatic effect on the microstructure, producing a change in morphology from equiaxed grains to a dendritic structure which was surrounded by a large fraction of a second phase (Fig. 3). This second phase was determined to be Sm_2C_3 from x-ray diffraction analysis.

The magnetic properties were strongly dependent on the microstructures. In the binary (unalloyed) SmCo_x alloys, the coercivity was significantly affected not so much on the

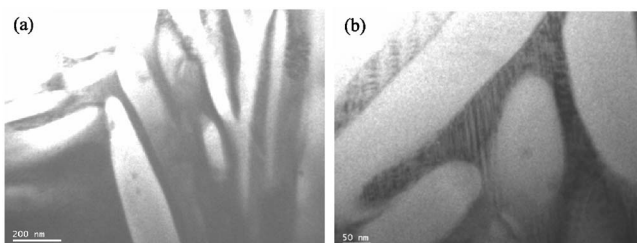


FIG. 3. Transmission electron micrographs revealing the microstructure of the $(\text{Sm}_{0.12}\text{Co}_{0.88})_{95}\text{C}_5$ alloy melt spun at 40 m/s showing (a) dendritic structures and (b) the second phase, Sm_2C_3 in the interdendritic region.

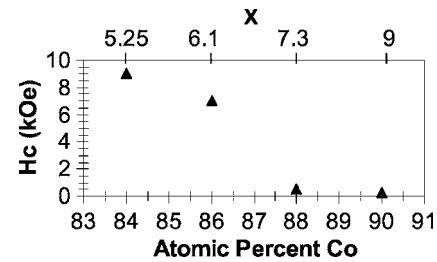


FIG. 4. Relationship between at. % Co and intrinsic coercivity for the SmCo_x alloys –40 m/s.

Sm/Co ratio but on the phase formation. The lack of dependence on Sm/Co ratio was somewhat surprising, given the strong dependence of coercivity on the Sm/Co ratio in $\text{Sm}-\text{Co}-\text{Nb}-\text{C}$ alloys.⁹ Here, a dramatic decrease in coercivity coincided with the formation of Co (Fig. 4). The $\sim 80 \text{ nm}$ fcc Co evidently enables reversal, which reduces the coercivity. Interestingly, the $x=6.1$ and 5.25 alloys had rather high coercivities, especially considering the rather coarse grains which may exceed the single-domain limit for these compounds.

The addition of 3 at. % Nb or C significantly improved the coercivity of the SmCo_x with $x=7.3$ (Fig. 5). Additionally, the energy products were improved to 6–8 MGOe, excellent values for isotropic $\text{Sm}-\text{Co}$ -based permanent magnets. The improved coercivity is due to the concomitant reduction in grain size. The increase in the C-added alloy is also due to the formation of the grain boundary phase, which effectively isolates the hard magnetic grains from one another. This is also readily evident in the alloy with 5 at. % C, which had a coercivity of 37 kOe. The dramatic increase here is due to the decreased magnetostatic interactions between the well-isolated SmCo_7 grains.

CONCLUSIONS

The binary SmCo melt-spun ribbons can achieve better microstructures and magnetic properties when modified with Nb and C additions. The addition of Nb helps to reduce the size of the (1:7) phase and thus helps to improve coercivity. The addition of C results in morphological changes in the microstructure which reveals the source of high coercivity, the isolated smooth interfaces. The intergranular region of

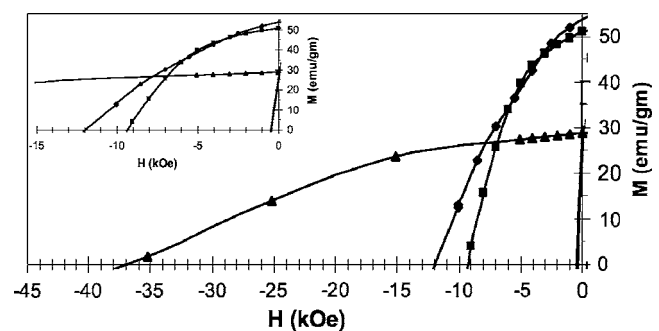


FIG. 5. Demagnetization curves for the $(\text{SmCo}_{7.3})_{100-y}\text{T}_y$ –40 m/s alloys at different T and y values: $T=\text{Nb}$ and $y=3$ (\blacksquare), $T=\text{C}$ and $y=3$ (\blacklozenge), and $T=\text{C}$ and $y=5$ (\blacktriangle). The curve (—) is indicating the sample without any additive. The inset shows an expanded view of the region from 0 kOe to –15 kOe.

the grain boundary contains a different phase that separates the grains and thus lowers the magnetostatic energy resulting in the higher coercivity.

ACKNOWLEDGMENTS

This project was supported by the National Science Foundation under Grant No. DMR0305354. The authors also benefited greatly from the shared facilities at the University of Nebraska's Materials Research Science and Engineering Center, QSPINS, funded by the National Science Foundation. Support from the Nebraska Research Initiative is also greatly appreciated.

- ¹W. Gong and B. M. Ma, *J. Appl. Phys.* **85**, 4657 (1999).
- ²A. Yan, O. Gutfleisich, A. Handstein, T. Gemming, and K.-H. Müller, *J. Appl. Phys.* **93**, 7975 (2003).
- ³A. Yan, A. Bollero, K. H. Müller, and O. Gutfleisich, *Appl. Phys. Lett.* **80**, 1243 (2002).
- ⁴A. Yan, A. Bollero, K. H. Müller, and O. Gutfleisich, *J. Appl. Phys.* **91**, 8825 (2002).
- ⁵S. S. Makridis, G. Litsardakis, I. Panagiotopoulos, D. Niarchos, Y. Zhang, and G. C. Hadjipanayis, *IEEE Trans. Magn.* **38**, 2922 (2002).
- ⁶S. S. Makridis, G. Litsardakis, I. Panagiotopoulos, D. Niarchos, and G. C. Hadjipanayis, *J. Appl. Phys.* **91**, 7899 (2002).
- ⁷C. H. Chen, S. Kodat, M. H. Walmer, S.-F. Cheng, M. A. Willard, and V. G. Harris, *J. Appl. Phys.* **93**, 7966 (2003).
- ⁸V. K. Ravindran, MS thesis, University Of Nebraska-Lincoln, 2005.
- ⁹S. Aich and J. E. Shield, *J. Magn. Magn. Mater.* **279**, 76 (2004).